ENGINEERING ANALYSIS OF THE TRANSMISSION OF RESPIRATORY DISEASES THROUGH THE AIR

Raimundo Nonato Calazans Duarte
Federal University of Campina Grande; Av Aprigio Veloso, 882 – 58.109-970 – Campina Grande/PB – Brasil
rnduarte@dem.ufpb.br

César José Deschamps
Federal University of Santa Catarina; Campus Universitário – Trindade – 88.040-900 – Florianópolis/SC – Brasil
deschamps@nrva.ufsc.br

Cezar Otaviano Ribeiro Negrão
Federal Centre of Technological Education of Parana; Av Sete de Setembro, 3165 – 80230-901 – Curitiba/PR – Brasil
negrao@cefetpr.br

Abstract. Aerial transmission of diseases has followed the man along all his existence and represents one of the most important ways to spread infectious respiratory illnesses. If someone suffering of influenza, for example, cough, sneeze, sing or even talk, small droplets containing microorganisms are expelled to the air. If some of these viable bio-contaminated droplets are inhaled and are deposited on a susceptive region of the respiratory tract, the disease may develop after human body immunologic defenses are surpassed. The process is almost the same for all the infectious respiratory diseases. However, deeper or alveolar deposition of the biological particles is needed for the installation of tuberculosis.The study of transmission has always been based on epidemiological and microbiological approaches. This paper describes an engineering viewpoint of aerial transmission of desease which involves multiple sub-processes such as bioaerosol discharge, aerosol transport, mass and heat interaction between particles and air, evolution of microbiological viability, droplets inhalation and deposition on the respiratory tract. As a result a semi-theoretical model is proposed. The airflow takes place in a two-dimensional room and it is modeled by a computational packag. The equations are solved for the gas phase (air and water vapor) and for the bioaerosol particles. The results include temperature, humidity and particle concentration fields. The risk of tuberculosis transmission of a potential TB host (the receptor) was analyzed.

Keywords: aerial transmission, tuberculosis, bioaerosol, respiratory diseases, indoor simulation.

1. Introduction

Human worries about aerial transmission of diseases are not new and medical investigations to avoid it remotes to a very far past. Lately, this problem has been under attention mainly because of the severe acute respiratory syndrome – SARS. The annual epidemics of influenza and the global increase of tuberculosis cases (Who, 1999) also reveal the great importance of such kind of disease dissemination.

Despite all medical research about the subject, technical publications concerning the engineering viewpoint about aerial transmission of diseases are very scarce. In a recent study (Duarte, 2001), a very wide review about this subject was conducted along with a detailed description of the processes involved. That work divided the transmission due respiratory aerosols in five parts: 1) Emission of the contaminated aerosol; 2) Transport of droplets through the air; 3) Heat and mass interaction between the bioaerossol and the air; 4) Time evolution of the microorganism viability; and 5) Inhalation and deposition of droplets on the respiratory tract.

Each one of these processes was studied and analyzed. From an engineering point of view, the three first processes are more familiar, but all of them are crucial to a proper formulation of the problem. Regarding the purposes of the present research, only the second and the third process were treated by computational fluid dynamics (CFD), while the others were modeled by empirical data. Duarte (2001) established the CFD code to solve the conservation equations (mass, momentum, energy, water vapor concentration) for the gas and discrete phase.

Lately, the model was described in detail and some implementations to the CFD package (Fluent, 2001) were performed (Duarte, Deschamps et Negrao, 2002a). These developments conducted to the first published results containing the temporal profiles of transmission risk (Duarte, Deschamps et Negrao, 2002b).

The current work describes the current state of the art and presents some new information. Firstly, the simplified indoor geometry and the basic characteristics of aerial transmission of diseases are described. The standard case is established by setting values to the parameters of the problem. These values mimic the architecture and installation of the University Hospital of the Federal University of Santa Catarina. The third and fourth sections describe, respectively, the formulation and some important details of the computation. Finally, the results are discussed.

2. Analyzed situation

For the sake of simplicity, a simple 2D geometry is considered to test the proposed formulation. This assessment avoided some computational shortcomings (low convergence rate; high instabilities and CPU cost; etc.) commonly observed in three-dimensional geometries. Besides, the paper focuses on the transmission modeling and not on computational fluid dynamics.

The analysis does not include some complexities observed inside buildings where the problem takes place. Therefore, the attention is on a contaminated person (source of contaminated particles) and a potential host in an indoor

environment. The air within the room is composed only of dry air and water vapor. Radioactive effects influencing the process were not considered in the present analysis.

As tuberculosis, caused by *Mycobacterium tuberculosis,* is one of the most dangerous infective diseases and due to its well-known pathology, it was chosen for the current study. On the other hand, influenza, for example, has multiple pathology agents and therefore its study may be complex.

2.1. Geometric characteristics

The computational domain is defined by the 2D geometry shown in Fig. (1). The air is supplied at the ceiling level and exhausted at the right hand side wall. The air supply direction is determined by an angle θ. The ill person (source of the bioaerosol) and the possible the new host are both represented by rectangular solid blocks whose surfaces are impermeable and isothermal. The dimensions (H_b and L_b) of such blocks have been derived from average anthropometric data. The aerosol source is located at H_r and x_e coordinates on the emitter block. The potential host works as a sink of particles which may be deposited on his respiratory tract. The only sources of heat and water vapor in the room are the two isothermal warm blocks (T_b). The walls, ceiling and floor are adiabatic.
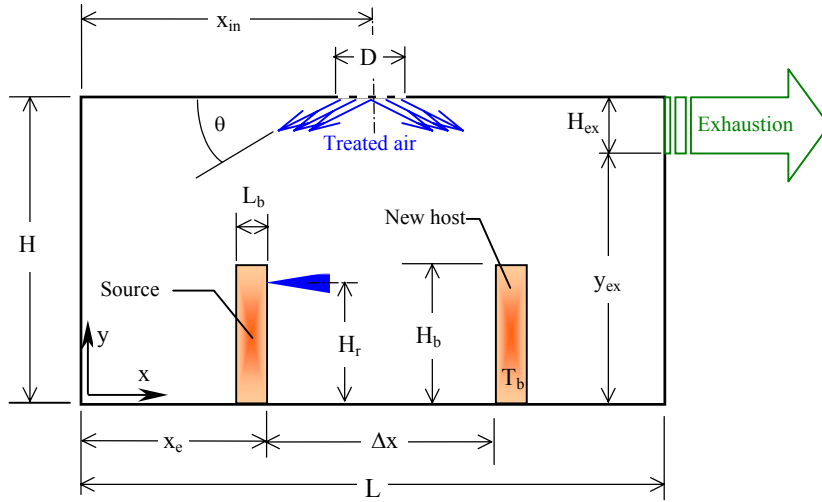

Figure 1. Geometry and computational domain.

2.2. The Standard case

The parameters of the problem were separated by groups according to their common characteristics: the geometric (H, L, x_{in}, D, y_{ex}, H_{ex}), operational (inlet speed - V_{in}, diffuser angle - θ, inlet relative humidity - ϕ_{in}, and inlet temperature -T_{in}, and distance between the persons - Δx), biological (size of spherical particles - d_p and concentration of microorganism in the respiratory fluid - $\bar{c}_r$) and physiological parameters (body temperature - T_b, humidity on the skin - ϕ_{sk}, temperature and humidity of the expired air - T_{resp} and ϕ_{resp}, inspiration rate of air - Q_{in}, production of respiratory particles and inhalation route of the contaminated aerosol (oral or nasal)). The inhalation route was based on empirical data and it influence was considered on the efficiency of particle alveolar deposition. This efficiency impacts directly on the microbiological dose accumulated in the lung and, so forth, the risk of contamination.

Although a respiratory aerosol, such as that produced by cough, is polydisperse (it presents several particle sizes) the bioaerosol is treated as monodisperse (a single d_p or $d_{p,mono}$). However, it can be easily changed to polydisperse.

Table 1. The standard case and its parameters

Category	Geometric						Operational				
Parameter	H (m)	L (m)	x_{in} (m)	D (m)	y_{ex} (m)	H_{ex} (m)	V_{in} (m/s)	θ (°)	T_{in} (°C)	ϕ_{in} (%)	Δx (m)
Standard Value	2.7	4.0	2.0	0.5	0.0	0.15	1.0	45	22	50	1.0
Category	Anthropometrical				Physiological						
Parameter	H_b (m)	H_r (m)	L_b (m)	Δy_{resp} (m)	T_b (°C)	ϕ_{sk} (%)	T_{resp} (°C)	ϕ_{resp} (%)	Q_{in} (l/min)	Event	Inhalation
Standard Value	1.7	1.6	0.25	0.02	33.7	80	37	100	30	Coughing	Oral
Category	Biological										
Parameter	$\bar{c}_r$ (ml^{-1})	d_p (µm)									
Standard Value	10^7	10									

The geometry specification also relies on the human body dimensions classified as anthropometrical parameters. The rectangular blocks simulating the room occupants were characterized by their height (H_b), width (L_b) and emission height (H_r). The later is equal to the position where particles are inhaled by the potential TB host. As mentioned before, the values attributed to these parameters arise from average anthropometric data of Brazilians (Kroemer, Kroemer et Kroemer-Elbert, 1997). Additionally, the section where the discharge and the inhalation of the bioaerossol occur, Δy_{resp}, was estimated by the authors. All this information can be found in Table (1).

3. Mathematical formulation

3.1. Particle dynamics

Mechanisms of different nature act on particles flowing within a fluid volume. Some of them are originated by fields (gravitational and electromagnetic, for example) that operate over the particle mass. Some others result from their own motion (drag, inertia of the displaced fluid, pressure field, among others). Finally, some of them appear as a result of the interaction with other particles (impact, interception, repulsion, attraction, etc). Random effects as thermophoresis, photophoresis and Brownian diffusion (Fuchs, 1964; Davies, 1966) can be important in the dispersion of submicrometric particles. As the effect of the later three may be small, the momentum conservation of the particle will include only inertia; aerodynamic drag and gravity, which are the dominant dynamic agents. Those interested on the details of the model should consult Duarte (2001).

3.2. Air-particle heat and mass interaction

The droplets in contact with the air are treated as spherical particles with symmetrical heat and mass transfers. In Fig. (2), T represents the absolute temperature (K), Y is the mass fraction of the water vapor in the gaseous mixture (kg_v/kg_{mist}) and the subscripts p, s, v and ∞ denote particle properties, particle surface, water vapor property and the gas, respectively. The environmental conditions are assumed known during the time intervals of the quasi-steady process of energy and mass transport from the particle.
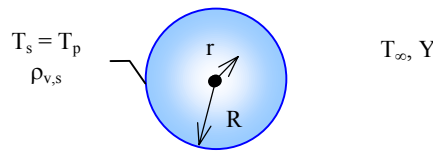

Figure 2. Liquid particle interacting with the gaseous atmosphere.

After the analyses of several models and the adoption of adequate simplifications, an approach was proposed for the interaction between the particles and the humid air (Duarte, 2001). The most important hypothesis are: i) the gas phase contains only air and water vapor; symmetric heat and mass transfer at particle surface; the properties are uniform inside the droplet; and absence of thermal radiation effects. Again, for concision of the present work, the conservation equations of particle mass, chemical species (water vapor) and energy are not shown in the present work. The details can be found in Duarte (2001).

3.3. Indoor convection

The most prominent characteristics of indoor air flows are the occurrence of turbulent three-dimensional jets (next to air supplies); the wide spectrum of flow regimes; the existence of internal barriers, partitions and other solid surfaces; the regions of strong recirculation; and the cells of natural convection.

Generally, the structure of the turbulent motion favors transport and fast diffusion of both scalar and vectorial quantities, justifying the need for detailed knowledge on the subject. On the analysis of thermal comfort and ventilation problems, for example temperature, humidity, speed and turbulence levels of air are important aspects. On the evaluation of indoor air quality and more particularly of aerosol transport, this importance is maintained or even magnified.

Regarding those aspects, an extensive literature review about the subject was carried out. This study includes turbulence modeling and computational code characteristics to reproduce this kind of flow. The results of this analysis were recently presented (Duarte, 2001) and indicate that the renormalization group (RNG) *k*–ε model is one of the most adequate for indoor air flows.

3.3.1. RNG *k*-ε turbulence model

According to some tests performed by Fluent (1995), the model is applicable to a wide variety of complex flows. It worked very well for separation and recirculation flows; curvilinear geometries, high speed gradients; heat transfer in low Prandtl fluids; low Reynolds number and transitional flows; eddies in main direction flows; secondary and

rotational flows; and coexistence of laminar and turbulent flows. These are the necessary capabilities for modeling indoor air flows.

The RNG k-ε turbulence model eliminates mathematically the smaller scales of turbulence, and the Navier-Stokes equations accounts for the large scales. In other words, transport equations are derived for the turbulent kinetic energy (k) and its dissipation (ε) and the constants of the model are mathematically obtained.

3.4. Risk of transmission

An important question comes to light: how the risk of transmission is related to the accumulated microbiological dose? The relationship depends on very complex aspects such as, the virulence, the deposited microbial population, the immunological state of the potential host, the site of deposition, etc.

Because of the lack of information, the risk of infection or transmission (R_{tb}) is simply related to the number of viable bacilli inhaled and deposited in the pulmonary region (D_{tb}) of a susceptible individual. To support this choice, some references on the subject were reviewed. The works normally analyze the environmental factors, the groups of risk and the risk due to biological pollutants in internal and external environments. Nicas' (2000) work deserves some attention for proposing an equation to evaluate the biological risk and for its efforts directed to *M. tuberculosis*.

One can infer that the deposited microbiological dose is directly proportional to the time of exposition to the contaminated atmosphere (Δt_{exp}), to the inhaled volume of air and to the particle concentration dragged by the air. Besides, the deposited fraction or efficiency of deposition [$\varphi=\varphi(d_p)$] on the respiratory tract and the viability of each particle (also function of d_p) also influence the risk of contracting the disease.

Nicas (2000) excessively simplified the estimation of D_{tb} assuming that only the concentration of microorganisms in the air is time dependent. The author also admits monodisperse aerosol composed by the bacillus itself, instead of particles, assumes lumped air around the source of particles and does not consider the decay of viability. In order to surpass these shortcomings, a previous work (Duarte, 2001) suggested a more accurate form to compute these dose, D_{tb}. Firstly, the monodisperse hypothesis is dropped and the respiratory aerosol is assumed to be composed of N classes of droplet sizes. The empirical data of Loudon et Roberts (1967; 1968) were employed to account for that. All the variables influencing the deposited microbiological dose are time dependent, but the volumetric respiratory rate (Q_{in}) and the initial concentration of microorganisms in the droplets. Therefore, the particle concentration of inhaled air, the viability and the deposition efficiency varies with time.

D_{tb} is thus a time integration of the deposited population for each class of particles, k. Naming the deposition of class k during this infinitesimal time by dD_{tb}^k, the following expression computes the microbiological dose accumulated in the lungs during a period of exposition, $\Delta t_{exp} = t_f - t_0$:

$$D_{tb} = \int \sum_{k=1}^{N} dD_{tb}^k = \int_{t_0}^{t_f} \sum_{k=1}^{N} \underbrace{\left[f_l^k(H_r,t)Q_{in} \right]}_{\substack{\text{Flow rate of classe k} \\ \text{particles}}} \times \underbrace{\left(\frac{N_t}{N_0} \overline{c}_r \right)}_{\text{Viable Fraction}} \times \varphi(d_p^k)\, dt = Q_{in}.\overline{c}_r \sum_{k=1}^{N} \left[\varphi^k \int_{t_0}^{t_f} f_{l,r}^k \exp(-K.t) dt \right] \quad (1)$$

where $f_l^k(H_r,t)$ or $f_{l,r}^k$ symbolizes the liquid fraction due to particle class k at the position of inhalation H_r and N_t/N_0 is the fraction of initial population of bacillus which is still viable. The volumetric flow rate, Q_{in}, is assumed constant and ranges from 6 to 7.5 liters/min. As Nicas (2000) suggested, the infection risk is determined by the exponential expression

$$R_{tb} = 1 - \exp(-D_{tb}) \quad (2)$$

As one can see, Equation (2) establishes zero risk when no deposition is observed and growing risk as the dose increases. One possible reason for choosing an exponential profile is the microbiological reproduction behavior. In appropriate conditions, each individual of a microbe population is able to produce another one, and together they create other four and so forth.

4. Computational details

4.1. Gas flow

For the continuous phase, the equations of RNG k-ε model were solved by the well-known finite volume method (Patankar, 1980). Differential equations are converted in a set of algebraic equations by dividing the time and spatial domains in a series of discrete regions. After applying linearization techniques, the resulting system of linear equations is solved by computational procedures. An implicit formulation is applied to the equations and they are solved iteratively to obtain the fields of pressure (P), velocity components (U and V), turbulent variables (k and ε), temperature (T) and mass fraction of the water vapor (Y).

The pressure-velocity coupling was carried out by the SIMPLEC algorithm also detailed by Patankar (1980) and the transient term was interpolated by a first-order approach (Fluent, 2001). After testing some alternatives available in the

computational package, a second order algorithm was applied to the pressure interpolation, while the power-law scheme was adopted for the other variables. For the turbulence variables, the non-equilibrium wall-functions were applied and the thermal buoyancy is considered as a source of both k and ε.

The strong coupling between the equations and the nonlinearities demanded the use of relaxation in all simulations. In addition to the primitive variables, the specific mass of the gas mixture, the terms of fluctuation, the turbulent viscosity and the source terms due to the discrete phase has to be relaxed. Without relaxation, the instabilities do not allow convergence. The coupling between the discrete and continuous phases is achieved by including source terms at the momentum, energy and water vapor equation for the gas, which are constantly recalculated as the particle position changes.

In order to establish the flow that would serve as initial condition to the aerosol, the buoyancy effect was progressively scaled up by controlling the value of the gravitational acceleration (g). Firstly, a pure forced convection (g = 0) condition is obtained and then the g is increased to a higher value. Usually, two intermediate values were necessary before the standard mixed convection (g=9.81 m/s^2) is achieved.

After the initial field has been established, the bioaerosol is emitted to the room by changing the solid boundary condition; saturated air and contaminated particles are released through the inlet section. To prevent an abrupt change of the boundary condition and therefore to avoid numerical instability, a strategy to control the rise of the air speed from zero to a typical speed (U_{emi}) is adopted. The procedure also controls the reduction of the air speed at end of the emission period. Fig. (3) illustrates the profile which defines the emission event. The constants "a" and "τ" are, respectively, 2.0 and 0.05s.
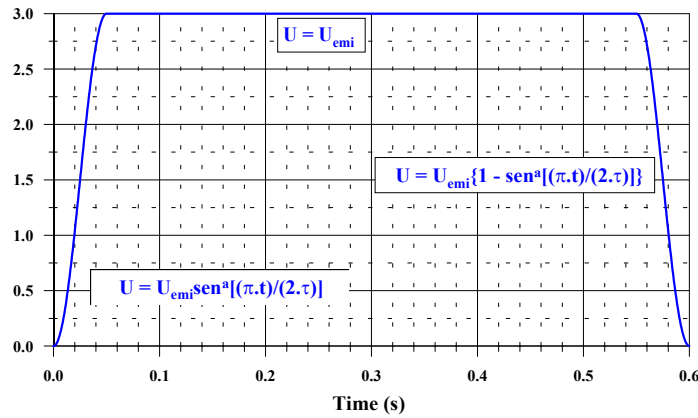

Figure 3. Profile used to graduate the air velocity during the bioaerossol emission.

As the computational code does not allow the use of the same strategy for the particle velocities, the emission of aerosol is initiated when the air speed reaches its maximum value U_{emi}. At this moment, the particles are released during a 0.5s period. After this period, the emission of particles ceases and the gradual reduction of the air velocity begins. This is acomplished by a profile similar to the growth, as illustrated in the Fig. (3). After 0.6 seconds, the solid boundary condition is completely reestabilished. For a single emission, the solution progresses until the microbiological dose and the risk of transmission (R_{tb}) achieves a steady state.

4.2. Particle motion

After the flow has been solved, the transient mean velocity, temperature and mass fraction fields for the continuous phase are available and the particle equations are thus solved by employing the local values of these variables in each cell of the mesh. The particle momentum equation allows the computation of the velocity inside each cell and the identification of its trajectory. To update the particle mass and temperature, a similar procedure is used by the computational code.

5.   Some results

Despite the small duration of a cough, the simulation takes place for about two hundred seconds. The solution used a maximum time-step of three seconds providing detailed information about the spread of particles in the room. As will be shown in section 5.4, the transmission process lasts for 5 to 10 seconds. As this information was unknown before the simulations, the computational solution was accomplished for about two hundred seconds.

The results are only for the standard case and their presentation was organized in four sections. The first shows the initial fields of the fundamental variables: the mean velocity, the temperature and the humidity of the gas phase. Although the problem is transient, these initial fields are decisive to explain the dynamics of the particles and, therefore, the transmission process. The next contains information about the aerosol volume fraction distribution. The later two

sections illustrate the fields of the accumulated microbiological dose (D_{tb}) in some critical instants and the temporal profiles of the risk, R_{tb}, respectively.

5.1. Fundamental variables

Before focusing the attention on the results for the already mentioned fundamental variables, a grid and residual sensitivity analyses were carried out for the equation of the continuous phase. Fifteen meshes were analyzed in order to verify the grid independence. Fig. (4) shows the selected grid.
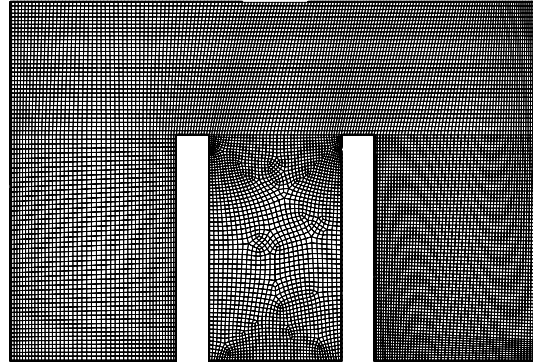

Figure 4. General aspect of the mesh employed.

As the particle dispersion is closely related to the transport phenomena, the property fields help the understanding of the liquid fraction and, therefore, the dose, D_{tb}, and the risk, R_{tb}, behaviors. The initial fields for these variables are depicted in Fig. (5) and Fig. (6).
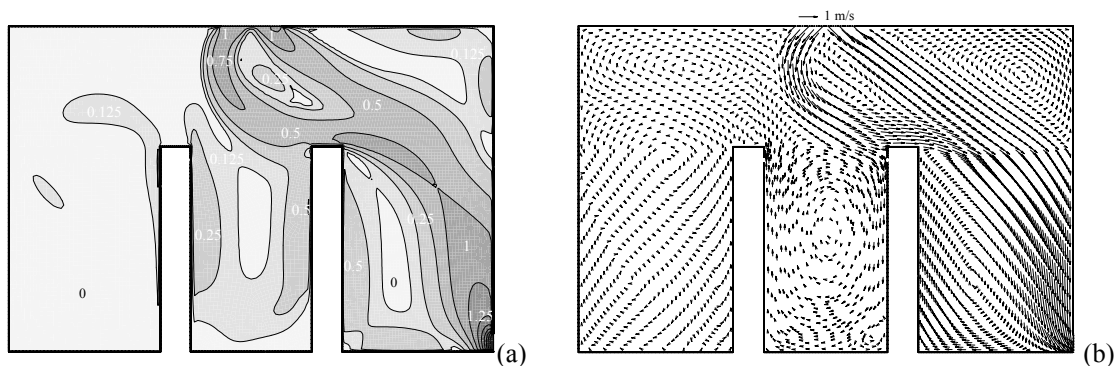

Figure 5. Initial velocity distribution [magnitude (a) and vector (b)].

By the images shown in Fig. (5), a typical indoor flow is observed. A main convective current is formed from the inlet section at the ceiling to the exhaust section down at the right wall. From now, this will be called ventilation current. The jet angle (θ) shows little importance over the air distribution in the room, once the left region of the domain remains almost stagnated.

Figure (5) also presents a downward forced flow (or deflected jet) next to the potential host overcoming the upward free convection. This is a characteristic of the two dimensional approach. In a real 3D situation, this flow would tend to pass aside the potential host towards the outlet and would be not directed to the floor. After flowing parallel to the floor, the flow changes its direction close to the left block (source of particles) and it is lifted by the upward buoyancy mechanism observed in that region. An almost closed recirculation cell is then created by this particular behavior of the 2D flow.
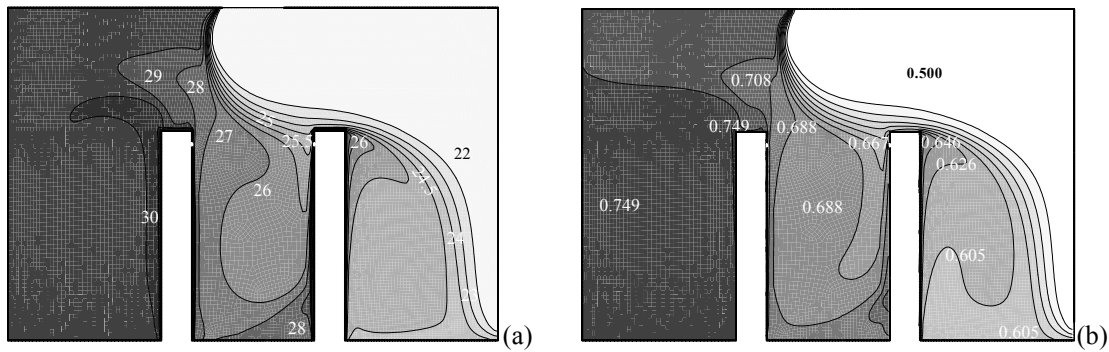
Figure 6. Isotherms (a) and humidity isolines (b).

The effect of the ventilation current and of the deflected jet over the temperature and humidity fields is evident, as shown by Fig. (6). As a consequence of the former, the inlet air properties are spread over the region where the current flows. Figure (6) also reveals a very low renovation of air between the source and the potential host and throughout the left part of the computational domain. Since the block surfaces are admitted isothermal and the air is almost saturated at that location [see T_b e ϕ_{sk} values at Tab. (1)], the temperature and humidity levels are dictated by the boundary conditions at these surfaces.

5.2. Aerosol volume fraction

A good way to follow the particle trajectories is to observe how the liquid mass fraction varies along the time. Defined as the volume ratio of aerosol and the mixture of gas and aerosol (whose volume is the same as the finite volume), this variable is directly related to the amount of particles inhaled (see Eq. (1)). In its evaluation, the computational code considers only those particles currently inside a certain finite volume.

The range of volume fraction is shown at the top of Figs. (7) and (8) and represents the limit values of such variable within the specified time. Figure (7) clearly demonstrates the high agglomeration of particles earlier after the aerosol discharge. As the standard case assumes monodisperse aerosol, the motion of all particles is similar and the aerosol appears as a single cloud that moves very regularly. The combined action of the cough and the deflected jet, near the source block, rotates the aerosol cloud in anti-clockwise direction as it moves upward.
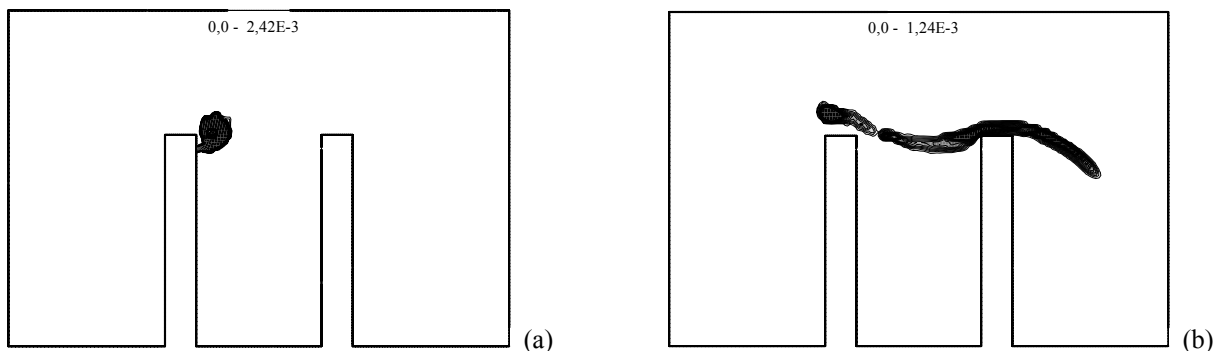

Figure 7. Aerosol mass fraction at t = 0.55 s (a) and 0.7 s (b).

As soon as the particle emission (t = 0.55 s) finishes, the ventilation current captures a great number of particles that pass over the potential host and is dragged towards the exhaustion (see Fig. (7b)). The remaining particles are deviated to the opposite direction by the upward current (due to the deflected jet) reducing significantly the quantity of particles near the potential host. This later aspect is clearly observed by comparing the maximum volume fraction at t = 0.7s with its counterparts at previous instants. There was approximately a 50% reduction.

About six seconds after the initial instant [Fig. (8a)], the maximum liquid fraction reduces to lower levels, partially because of the particle deposition on the surfaces of the domain and mainly because of the exhausting action of the ventilation current. This image also shows the action of the ventilation current impelling contaminated aerosol in the direction of the respiratory region (y ~ H_r) of the potential host. This portion of the aerosol is also under the influence of the deflected jet that tends to remove it from the respiratory region towards the floor. Figure (8a) also reveals that these particles follow the deflected jet in the direction to the source block. It moves upward and seems to be incorporated in a recirculation cell in the leftmost region of the domain, as shown by Figs. (8a) and (8b). These comments and the fields of Figs. (8b) and (8c) confirm the drag predominance over the gravitational deposition for the considered particle size (10 μm). The aerosol movement follows strictly the convective currents as shown by the figures.
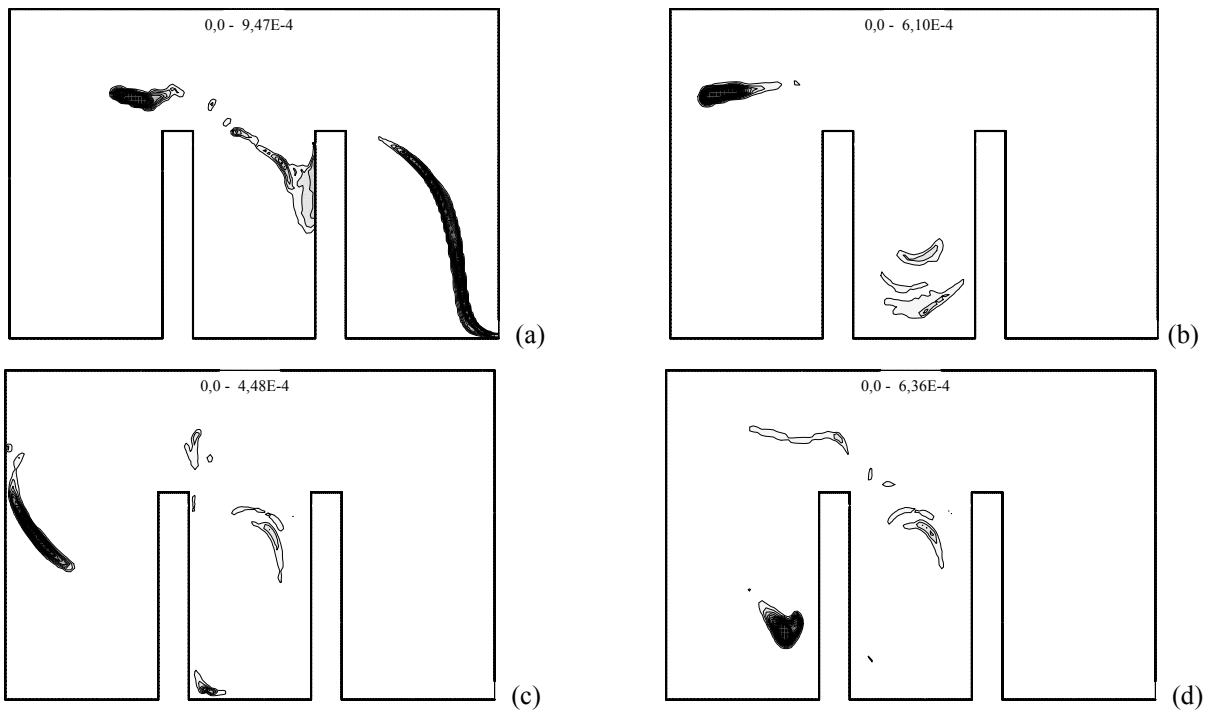
Figure 8. Aerosol mass fraction at t = 5.86 s (a), 10.22 s (b), t = 19.22 s (c) and 31.22 s (d).

The Fig. (8d) corroborates the effects observed at the other instants. An exception is the maximum liquid fraction that curiously presents a greater value in comparison with the previous instants. This is attributed to the high particle concentration behind the source block; a region of very weak flow and hence of low particle dispersion.

5.3. Acumulated microbiological dose

Before evaluating the next figures, two essential aspects of the microbiological dose, D_{tb}, are discussed: its cumulative and potential nature. Regarding the cumulative nature, D_{tb} is calculated by adding any bacillus deposited in the lung tract to those previously captured there.
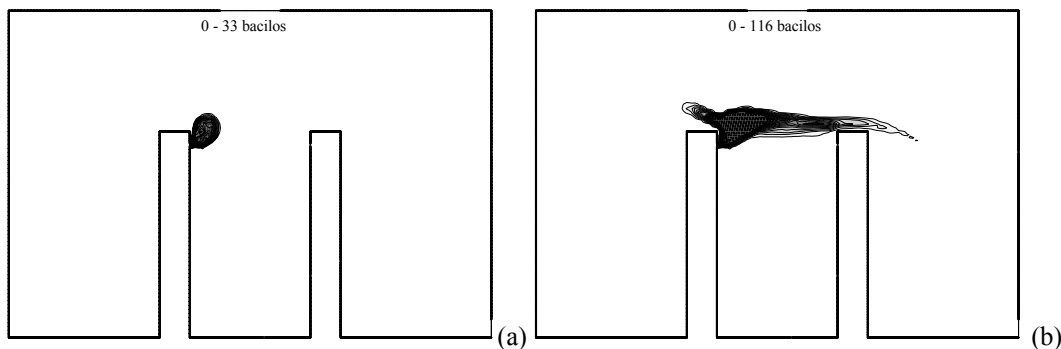

Figure 9. Microbiological dose distribution at t = 0.55 s (a) and 0.7 s (b).

In respect of potential nature, D_{tb} was evaluated in every grid cell of the domain, even though some of them do not represent points where the particles are inhaled. At the respiratory region of the potential host, the calculated D_{tb} is more realistic since there is a real process of inhalation there. As a particle can flow through a finite volume more than once, regions of recirculation tend to present higher levels of D_{tb}.

As the dose is a cumulative parameter, there is no surprise that the values of D_{tb} always increase with time. At the end of the aerosol discharge (t = 0.55 s), the maximum dose was 33 bacillus [Fig. (9a)] and, less than two seconds later, it raised to 116 [Fig. (9b)]. This growing evolution continued until 124 bacillus is reached, after approximately twenty seconds.
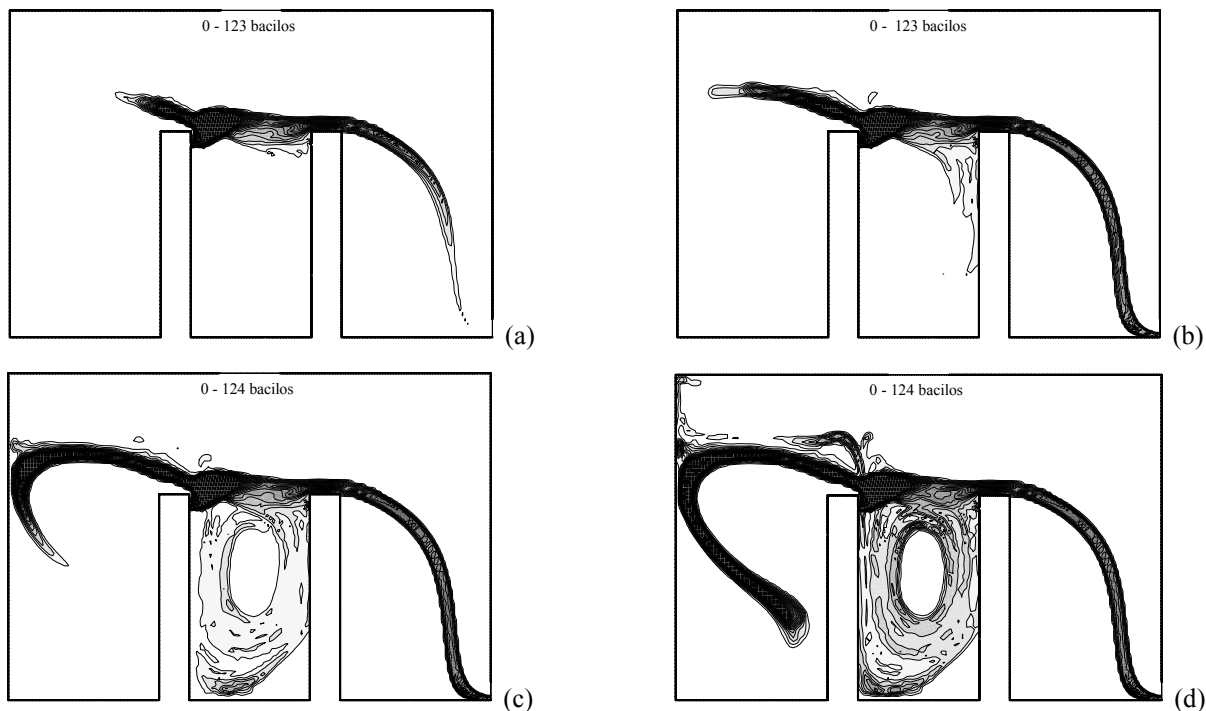
Figure 10. D_{tb} fields at t = 5.86 s (a), 10.22 s (b), 19.22 s (c) and 31.22 s (d).

Comparing Fig. (9) with Fig. (7), one can see the strong relationship between the microbiological dose and the aerosol movement inside the room mainly at earlier instants. As the particles spread over the environment and the recirculation effect begins to alter the D_{tb} values, this similarity desapears.

Figure (10) also reveals an excellent application of the D_{tb} fields. Since it is cumulative, these distributions are an interesting way to recognize the regions visited by the particles. Higher D_{tb} values (darker regions in the pictures) identify points where the particles either present high concentration or pass more than once.

5.4. Risk of TB transmission

Since the risk, R_{tb}, is directly related to the D_{tb} values [Eq. (2)], the risk distribution is identical to the dose one. Fig. 11 illustrates a time change of risk at a potential host position. As can be seen, the transmission process lasts no more than ten seconds and remains constant for the rest of the time. After five seconds of the discharge moment, the particles reach the potential host respiratory area and the transmission risk rises. Between the fifth and the tenth seconds, the R_{tb} value increases quickly and achieves its permanent value of 48 %.
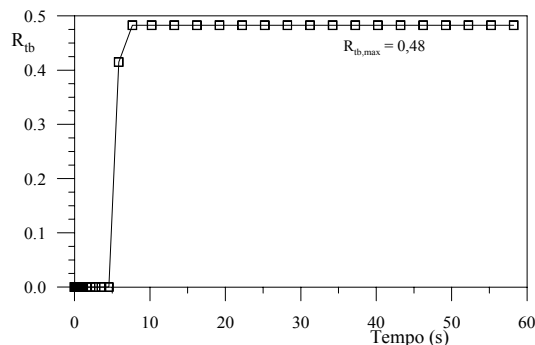

Figure 11. Transient profile of the risk index, R_{tb}, for the new TB host.

5. Acknowledgement

The authors would like to thank the Brazilian agency CAPES that supported this work.

6. References

Duarte, R. N. C., 2001, "Dispersão de aerossóis humanos contaminados em interiores", Thesis Proposal, POSMEC/UFSC, Florianópolis/SC, Brasil, 195 p.

Duarte, R. N. C., Deschamps, C. J. et Negrão, C. O. R., 2002a, "Modeling of tuberculosis transmission through respiratory aerosols", 1st Annual Workshop of Brazilian Tuberculosis Research Network, Rio de Janeiro/RJ, Brasil.

Duarte, R. N. C., Deschamps, C. J. et Negrão, C. O. R., 2002b, "A model for the disease transmission via bioaerosols", Proceedings of the 9th Brazilian Congress of Thermal Engineering and Sciences (Compact Disk – ISBN 85-87978-03-9), Paper CIT02-0390, Caxambu/MG, Brasil.

Fluent, 1995, "FLUENT 4.3 User's guide", Fluent Inc., Lebanon/NH, USA.

Fluent, 2001, "FLUENT 6.0 User's guide", Fluent Inc., Lebanon/NH, USA.

Kroemer, K. H. E.; Kroemer, H. J. et Kroemer-Elbert, K. E., 1997, "Engineering physiology: bases of human factors/ergonomics", 3rd Edition, Van Nostrand Reinhold, New York, USA.

Loudon, R. G. et Roberts, R. M., 1967, "Droplet expusion from the respiratory tract", Am. Rev. Resp. Dis., Vol. 95, pp. 435-442.

Loudon, R. G. et Roberts, R. M., 1968, "Singing and the dissemination of tuberculosis", Am. Rev. Resp. Dis., Vol. 98, pp. 297-300.

Nicas, M., 2000, "Markov modeling of contaminant concentrations in indoor air", AIHA J., Vol.. 61, No. 7, pp. 484-491.

Patankar, S. H., 1980, "Numerical heat transfer and fluid flow", Hemisphere Publishing Corp., New York, USA.

Who, 1999, "The world health report 1999", World Health Organization, Geneve, Switzerland, 121 p.

6. Copyright Notice